Pharmaceutical Science Advances 1 (2023) 100011

Contents lists available at ScienceDirect

Pharmaceutical Science Advances

journal homepage: www.journals.elsevier.com/pharmaceutical-science-advances

Ab initio modeling and ligand docking of quercetin and the MC-LR transporter protein Oatp1b2/OATP1B3

Kriti Shrinet [a,b], Ritika K. Singh [a], Riden Saxena [c], Avinash K. Chaurasia [a], Arvind Kumar [a,*]

[a] School of Biotechnology, Institute of Science, Banaras Hindu University, Varanasi, Uttar Pradesh, 221005, India
[b] School of Biotechnology, IFTM University, Moradabad, Uttar Pradesh, 244102, India
[c] Department of Obstetrics and Gynecology, Institute of Medical Sciences, Banaras Hindu University, Varanasi, Uttar Pradesh, 221005, India

ARTICLE INFO

Keywords:
Cyanotoxin
Quercetin
Modeling
Inhibitor
Transmembrane proteins
Transporter protein

ABSTRACT

Trans-membrane proteins (TMPs) play a crucial role in the translocation of organic and inorganic molecules. Unlike other proteins, TMPs are difficult to model structurally because of their location within the amphipathic plasma membrane. In this study, we focused on examining the transport of the cyanotoxin microcystin-LR (MC-LR) through organic ion transporting polypeptides (OATPs) and whether the bioactive phytoconstituent quercetin can function as a barrier to the transportation of MC-LR. To test this hypothesis, we first modeled the transporters OATP1B3 and Oatp1b2 localized in the human and mouse liver, respectively, by *ab initio* modeling with the Iterative Threading ASSEmbly Refinement server and refined the generated model using the refinement tool of the ModLoop server. Using different tools and servers, the structural quality of the transmembrane helices was validated and found to be an accurate structure of a TMP. Docking analysis was performed with the ligands MC-LR and quercetin with both OATPs using the PatchDock and FireDock online servers. The results, in the form of the global energy of both docked structures, were based on predictions made earlier. The Oatp1b2 global energy for quercetin was −36.4 kcal/mol, compared with the corresponding value at the MC-LR location which was only −5.59 kcal/mol. Similarly, in the case of OATP1B3 with quercetin, the global energy was found to be −39.0 kcal/mol, whereas with MC-LR it was −15.6 kcal/mol. These results clearly show that quercetin competitively inhibits the binding of MC-LR to its respective targets.

1. Introduction

Trans-membrane proteins (TMPs) participate in the maintenance of normal cell function, cellular signaling, activation of the immune system, and energy generation from ATP [1]. TMPs assist in the translocation of endogenous and exogenous compounds, xenobiotics, and drugs across the plasma membrane. More than 50% of known TMPs are research targets in the ongoing development of different drugs, antibiotics, and chemotherapeutics. Human and rodent organic anion transporter polypeptides (OATP) are TMPs of a subgroup of transporters that belong to a superfamily known as solute carrier organic transporters (SLC21), encoded by SLCO genes. Humans and mice have 11 and 15OATPs, respectively, which are reported to function in a sodium- and ATP-independent manner on endogenous substrates, such as bile acids, steroid hormone conjugates, thyroid hormones, prostaglandins, cyclic nucleotides, xenobiotics, eicosanoids, peptides, and numerous drugs, in many tissues [2,3]. The genes Oatp1a1, Oatp1a4, Oatp1b2, and Oatp2b1 are expressed in the liver of mice and OATP1B1, OATP1B3, and OATP2B1 are expressed in hepatocytes of the normal human liver [4]. Mouse Oatp1b2 is an ortholog of OATP1B1 and OATP1B3 in humans, and all three are specifically and highly expressed in the liver. OATP1B1 and OATP1B3 are localized on the basolateral membrane of hepatocytes, and OATP1B3 is primarily expressed around the central vein of hepatic lobules [2,5]. OATPs and their polymorphic variants are functional in the hepatobiliary excretion and transport of different drugs and toxins. Owing to these properties, OATPs are thought to have potential as agents to increase the intrahepatic concentration of drugs targeting the liver, with the current research focus being drug efficacy or toxicity in drug-drug interactions. Microcystins, a class of toxins produced by certain species of cyanobacteria, are hepatotoxic to both humans and animals and cause severe liver injury upon both acute and chronic exposure in dose-dependent conditions [6]. The toxic effect of microcystin LR (MC-LR) first came to light in 1996, when an unfortunate medical accident in Brazil resulted in the death of 76 patients with kidney

* Corresponding author.
E-mail addresses: arvindkumararvind8@gmail.com, k_arvindk@rediffmail.com, arvindk@bhu.ac.in (A. Kumar).

https://doi.org/10.1016/j.pscia.2023.100011
Received 5 April 2023; Received in revised form 7 June 2023; Accepted 13 June 2023

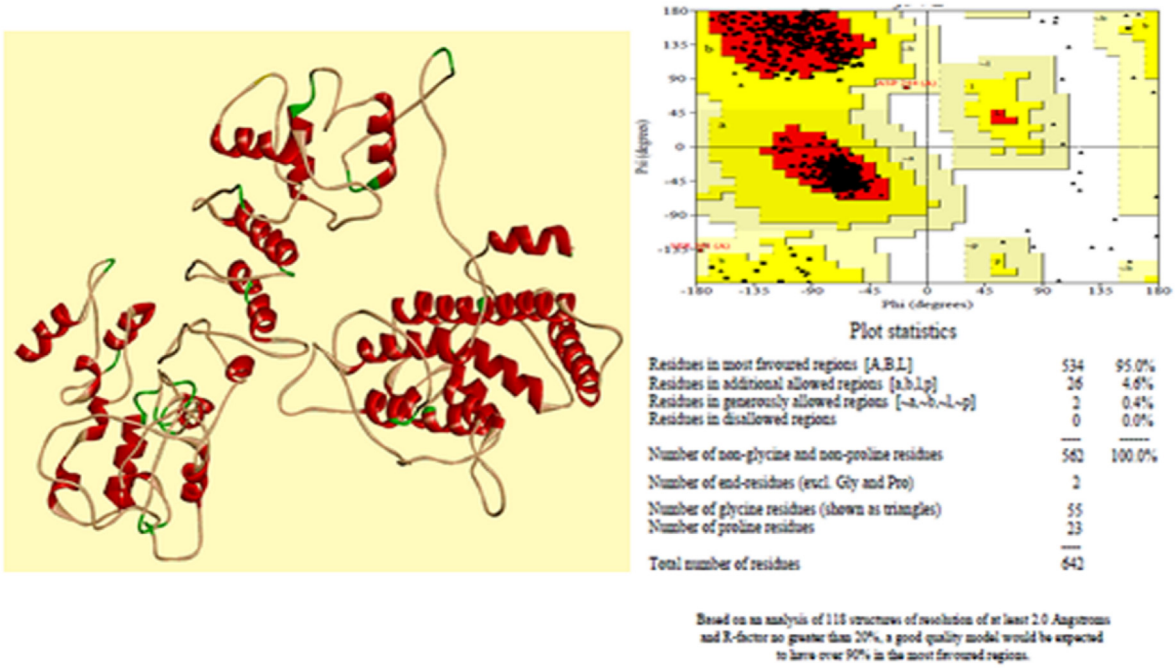

Fig. 1. Model structure of the OATP1B3 protein along with its Ramachandran plot.

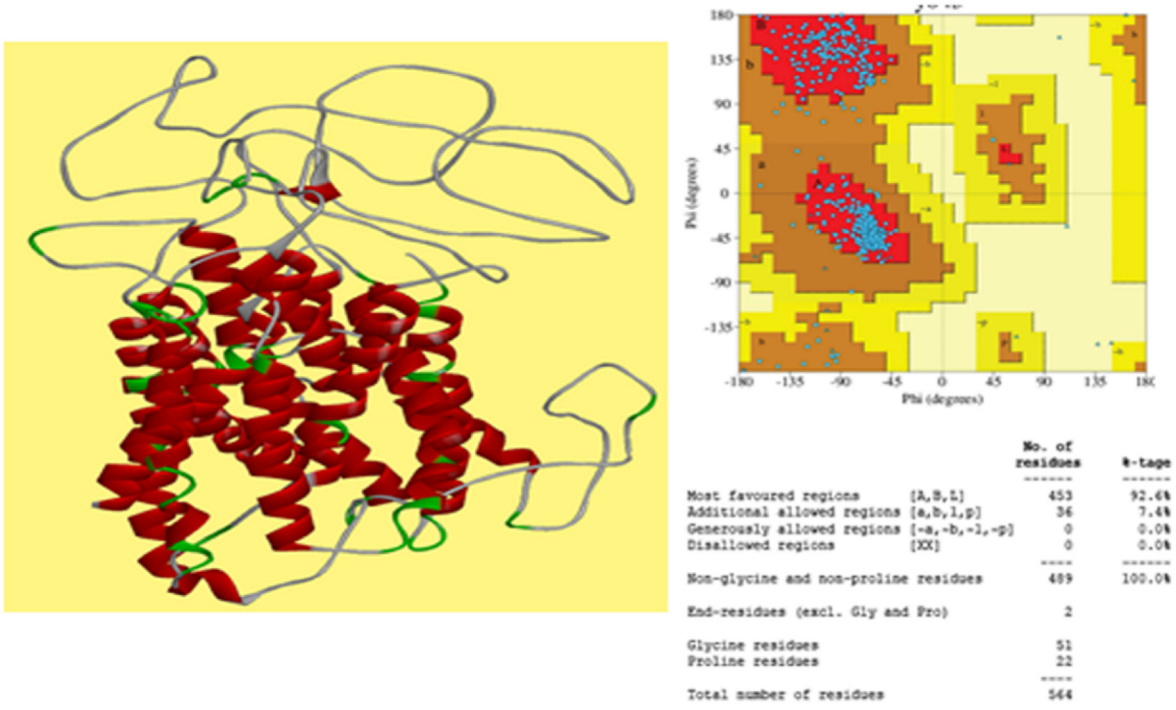

Fig. 2. Model structure of the OATB1b2 protein along with its Ramachandran plot.

failure who were undergoing hemodialysis and were exposed to microcystin-contaminated water [7]. To date, more than 130 variants of microcystins have been characterized, among which MC-LR is the most potent and widely distributed. Organic anion transporters, specifically OATP1B1 and OATP1B3 in humans, and Oatp1b2 assist in the cellular uptake of MC-LR and induce inhibition of protein phosphatases PP2A and PP1, increase ROS, and deplete the level of cellular GSH [8,9]. Oatp1b2 (−/−) knockout mice with normal phenotypes were completely resistant to microcystin-LR-induced hepatotoxicity. This shows that Oatp1b2 and probably its orthologs OATP1B1 and OATP1B3 are good targets for investigating the role of these transporters in toxins and counteracting drug disposition and hepatotoxicity [10]. Therefore, these genes are of great interest as targets for drug delivery, metabolism, transporter inhibition, and overexpression because of their crucial role in the transport of molecules and as receptor switches. Membrane proteins are currently the focus of research, because most drugs target this transporter to enter the cell [11]. In 1984, the first three-dimensional (3D) atomic structure of a membrane protein was experimentally formulated [12], but the structures of more proteins are still unknown. Protein structure modeling is tedious and requires both experimental and computational approaches.

Table 1
Statistical analysis of Secondary structures, H bond and Volume measures of OATP1B3 and Oatp1b2 model protein.

	OATP1B3			Oatp1b2		
	Statistic	Observed	Expected	Statistic	Observed	Expected
Secondary structures	Helix	258 (40%)	-	Helix	276 (48%)	-
	Beta	9 (1%)	-	Beta	6 (1%)	-
	Coil	375 (58%)	-	Coil	282 (50%)	-
	Turn	112 (17%)	-	Turn	120 (21%)	-
Hydrogen bonds	Mean H-bonddistance	2.3 sd = 0.4	2.2 sd = 0.4	Mean H-bonddistance	2.3 sd = 0.4	2.2 sd = 0.4
	Mean H-bond energy	−1.4 sd = 1.0	−2.0 sd = 0.8	Mean H-bond energy	−1.6 sd = 1.1	−2.0 sd = 0.8
	Res. with H bonds	350 (54%)	481 (75%)	Res. with H bonds	360 (63%)	423 (75%)
Volume measures	Total volume (packing)	96293.3 Angs**3	85950.3 Angs**3	Total volume (packing)	82080.4 Angs**3	76114.4 Angs**3
	Mean residue volume	150.0 sd = 64.7	125.0 sd = 40.0	Mean residue volume	145.5 sd = 50.3	125.0 sd = 40.0
	Mean frac volume	1.1 sd = 0.4	1.0 sd = 0.1	Mean frac volume	1.1 sd = 0.3	1.0 sd = 0.1
	Molecular weight	70575.46	–	Molecular weight	62559.29	–

In recent years, membrane protein structures were resolved with the use of X-ray crystallography or NMR spectroscopy, but their numbers are still very low as compared to soluble protein structures, which are approximately 1% of all protein structures in PDB [13]. TMPs span the plasma membrane; therefore, it is technically difficult to isolate, synthesize, solubilize, and maintain functional stability in the tertiary/quaternary structures of TMPs during the process of crystallization before X-ray crystallography [14,15]. New crystallization methodologies and high throughput technologies like miniaturization, integration, third-generation synchrotrons, electron microscopy help generate good protein structures; however, there are information gaps in 3D structural datasets, such as CryoEM map [13,16,17]. To fill these informational gaps, numerous rapid and low-cost computational strategies have been developed [18,19].

To date, the structures of only 14 members of solute carrier (SLC) superfamily have been determined (using X-ray methods). Approximately 15,100 human genes are currently annotated as transport proteins, some of which have been sequenced [13]. Among all the families of SLC, organic anion transporter proteins (OATP/OAT) are the most abundant and frequently targeted in current research because of their roles in the uptake of drugs and as tumor biomarkers [20–22]. Therefore, when only information regarding tissue expression, protein sequence, ligand-based experiments without synthesized proteins, and gene annotation for proteins is available, computational approaches are the only solution.

In terms of various human cancers, such as lung, colon, and pancreatic cancers, there is high expression of the isoform of OATP1B3, known as Cancer-type OATP (Ct-OATP). This specific isoform is generated by translation occurring at three out of four open reading frames, the transcription start site, and an alternative promoter region, localized at intron 2 of OATP also play crucial roles. OATP and its role in cancer prognosis and clinical outcomes is a topic for future research [23], which would require structural 3D models that help infer the substrate specificity of OATP as well as its functional and mechanistic significance.

Oatp1b2 (76.59 kDa) and OATP1B3 (77.27 kDa) are TMPs with 689 and 702 amino acids, respectively, translated from a 3307 and 3,014bp long mRNA sequences (NCBI Gene ID: 28253 and 28234). The protein sequence of Oatp1b2 (UniprotKB/SwissProt ID Q9JJL3.1) showed 66% identity and 98% query coverage with OATP1B3 (UniprotKB/SwissProt ID Q9NPD5.1) on blast search. Greater than 40% of the amino acid sequence identity was found within the same family of OATPs/Oatps as OATP1, whereas ≥60% of the amino acid sequence is within the subfamilies called OATP1B3/Oatp1b2 [2].

Interestingly, OATPs have a conserved signature sequence of 13 amino acids (D-X-RW-(I, V)-GAWW-XG-(F, L)-L) at the border between extracellular loop 3 and TM 6. The position of this sequence at the TM interface combined with the presence of three highly conserved tryptophan residues suggests a potential role in stabilizing proteins within the membrane [24]. To date, only a patch of sequences predicted to encompass TM6 has been studied (A257, W258, W259, L260, N261, F262, and L263). Mutations in tryptophan 258, 259, and phenylalanine262 to alanine amino acids in OATP1B1 resulted in a significant decrease in transport, signifying its role in protein function [25].

Quercetin (3, 3′, 4′, 5, 7-pentahydroxyflavone) (C15H10O7) is an important flavonoid polyphenol. It is classified as a flavonol and is one of the six subclasses of flavonoid compounds. Quercetins, the most prevalent type of flavonoid, are found in a wide range of edible plants and are available at a low cost in the form of tablets. The results of various *in vitro* and animal models have demonstrated that quercetin has a wide range of physiological effects, including antioxidant, anti-inflammatory, immunomodulatory, and antiviral activity. Significant research has been conducted on its effects on lipid peroxidation, platelet aggregation, and capillary permeability, all of which result in cardioprotective and anticarcinogenic properties [26].

A comprehensive understanding of TMP structures and their functional mechanisms can have a substantial impact on drug development, ultimately leading to improved healthcare solutions. Thus, we aimed to carry out *in-silico* based methodologies to illuminate the 3D structures of OATP1B3 and Oatp1b2 of the OATP family of the SLC21superfamily and explored the potential of quercetin to function as a competitive barrier in the transportation of the cyanotoxin MC-LR through OATPs.

2. Methods

2.1. Sequence analysis, molecular structure characterization, and modeling

The 3D structures of *Mus musculus* Oatp1b2 and the Human OATP1B3 transporter protein were not available in the PDB database, and only the mRNA protein sequences were available in NCBI with protein accession numbers NP_065241.1 and UniprotKB/SwissProt ID Q9NPD5.1, respectively. Thus, few attempts have been made to determine the 3D structure of the above-mentioned transmembrane transporter proteins based on the *ab initio* modeling approach. A BLASTp search was also performed for protein sequence matches to SLCO family members in other organisms [27]. Protein sequences were used for modeling, docking, transmembrane structure determination, and visualization using the Discovery Studio 3.0 software [28]. For *ab initio* modeling, Iterative Threading ASSEmbly Refinement and Swiss Model (template-independent manner) servers were used to model this protein, given that no template has been found with significant similarity (<25%) with the target protein [29]. Iterative Threading ASSEmbly Refinement (I-TASSER) uses a combination of three conventional methods for structural modeling: comparative modeling, threading, and *ab initio* modeling [30]. Hence, this method is reliable for modeling structures of proteins with very little or no shared similarity, as evidenced by their primary sequences. We further verified the model using different servers and used it for docking with MC-LR and hepatoprotective bioactive compounds.

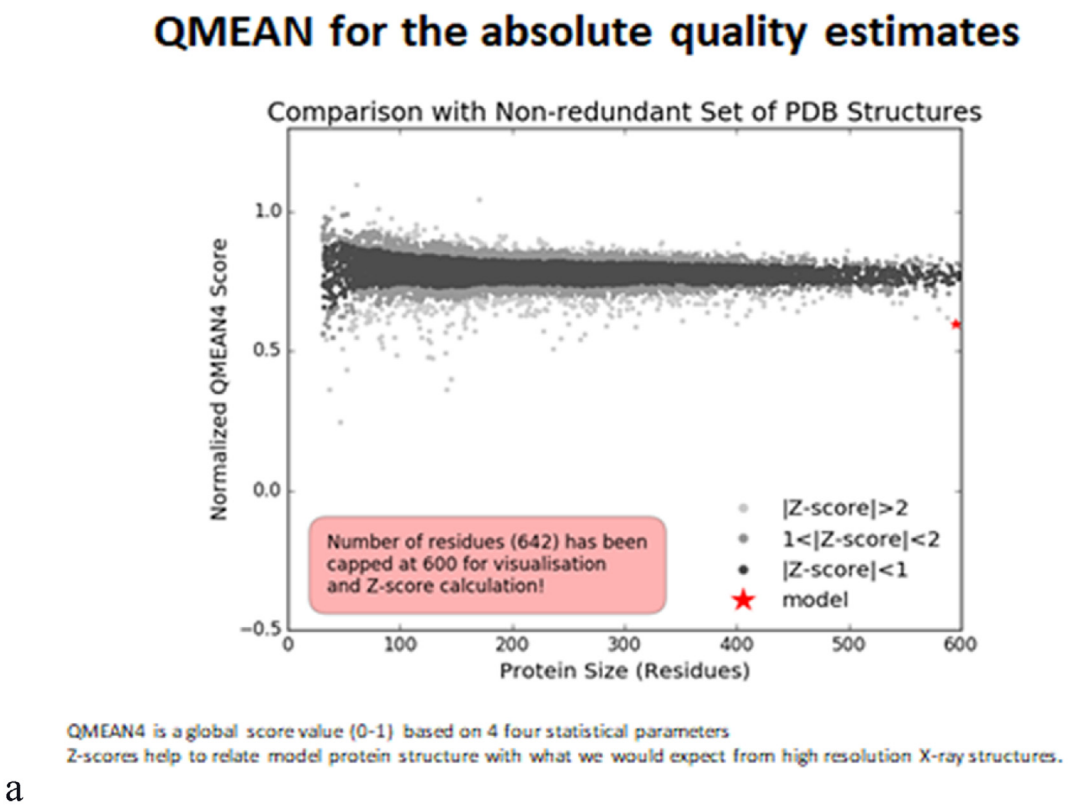

a

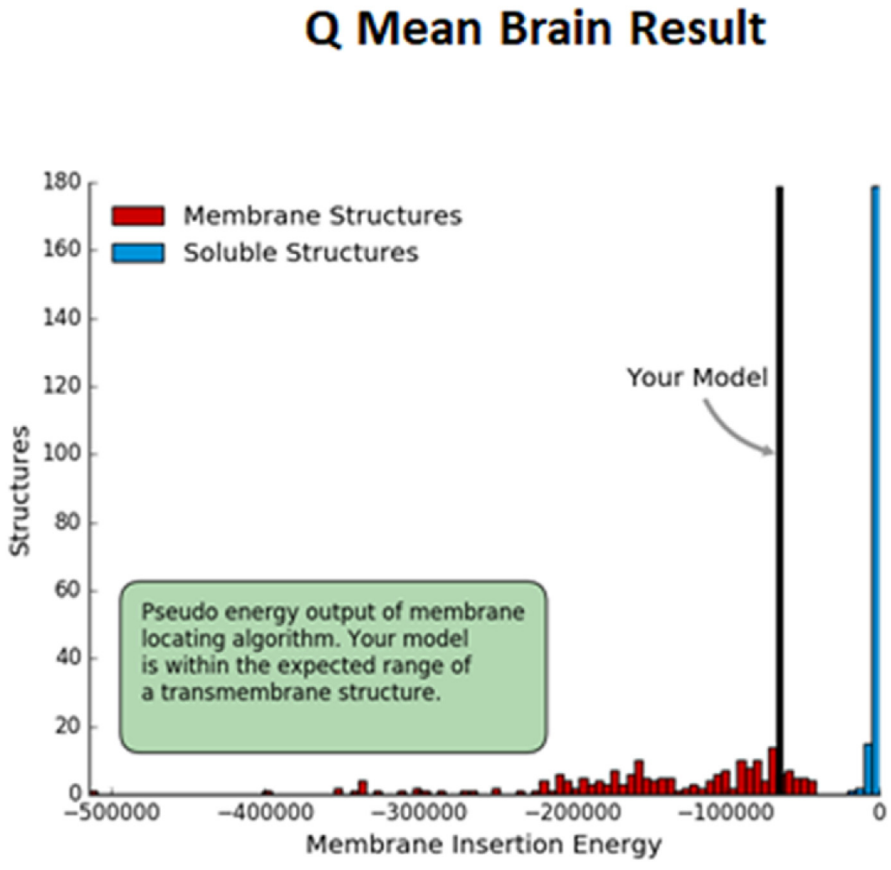

b

Fig. 3. a. OATPIB3 Model is lying near Z-score values, **b.** Model is lying in between the expected range of a trans-membrane structure.

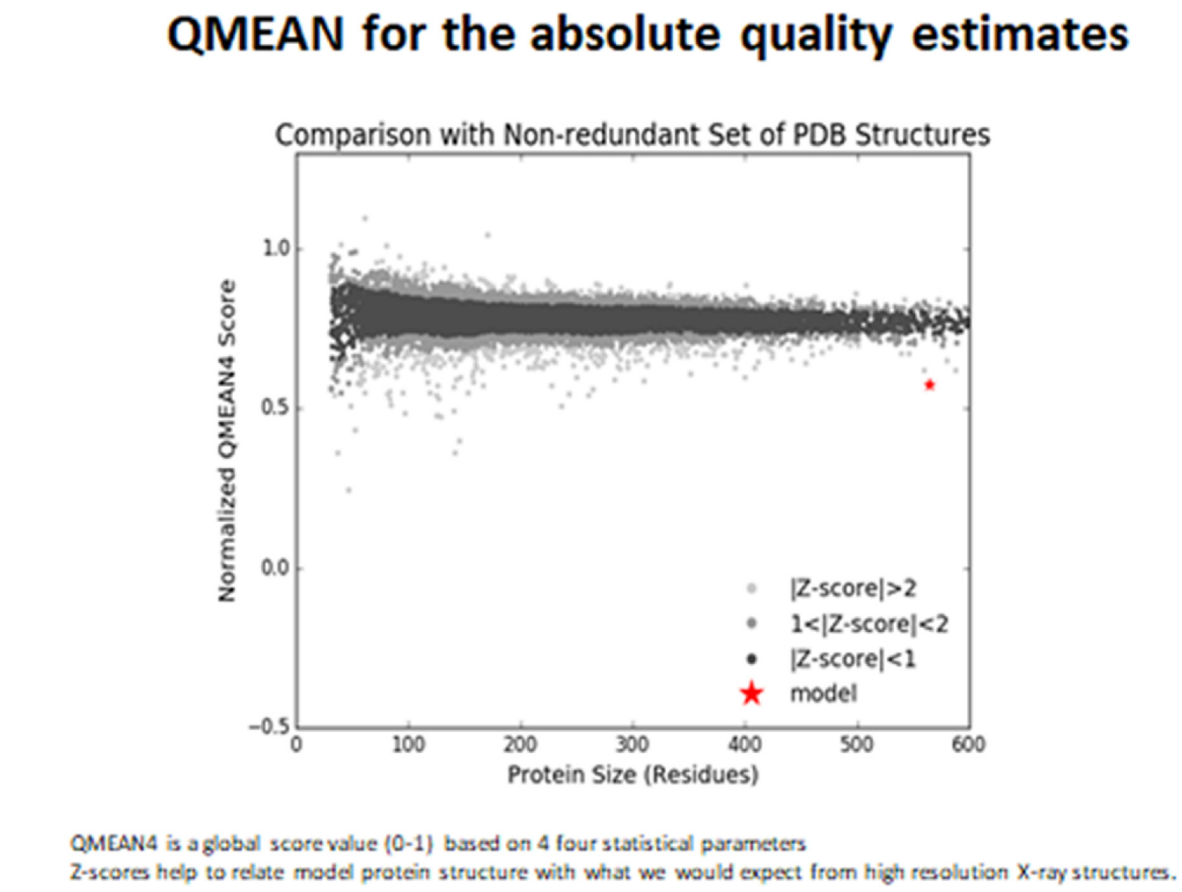

Fig. 4. **a**. OATPIb2 Model is lying very near to Z-score values, **b.** OATPIb2Model is lying in between the expected range of a trans-membrane structure.

2.2. Protein structure refinement through different options

To improve the structural integrity and unphysical local distortions, refinement of both models OATP1B3and Oatp1b2 was performed using the Modrefiner tool, which works on a composite physics and knowledge-based force field and essentially optimizes the structure by means of atomic-level energy minimization and physical constraints. This is a two-step process: the backbone atoms for the Cα trace are constructed, after which a simulation is run to refine the backbone structure. This process results in an improvement in both the global and local structures, with more accurate side-chain positions and better hydrogen-bonding networks [31]. For validation of both the models, the RAMPAGE tool was used which is based on Ramachandran plot analysis to visualize energetically favorable regions for amino acids backbone dihedral angles phi (ϕ) and psi (ψ) [32]. The model was refined manually because online refinement servers were not sufficiently helpful to produce significant changes in the model quality. This requires the Swiss PDB Viewer, a tool created for experimental scientists as a command-free, powerful, and

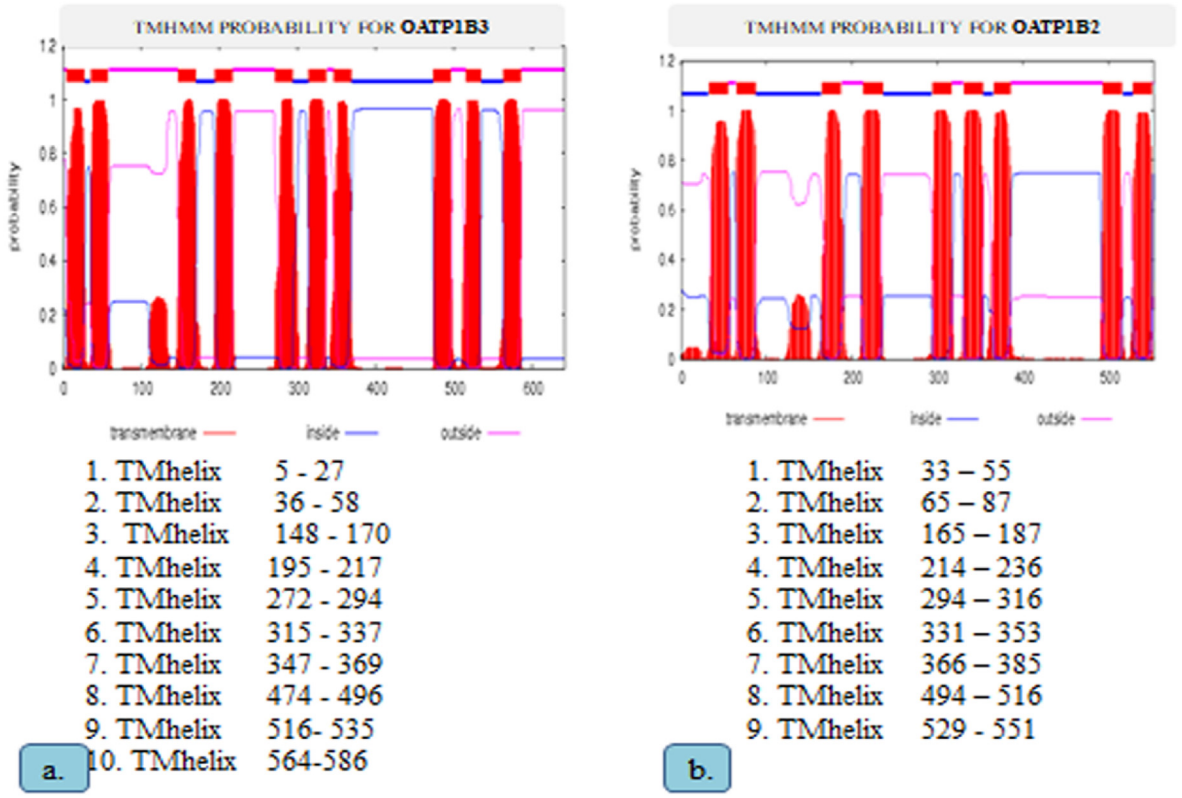

Fig. 5. a. showing TM-helixes for OATP1B3 protein **b**. showing TM-helixes for Oatp1b2 protein.

Table 2
Different orientation of the OATP1B3 protein with TM-scores.

Serial no	Inside to	Outside	Score	Outside to	Inside	Score
1.	8	27	952	8	28	1290
2.	36	61	1866	36	58	1656
3.	109	137	**419**	110	136	547
4.	155	174	1788	147	169	1841
5.	198	220	2393	196	220	2511
6.	280	300	2092	272	300	1843
7.	316	332	1819	316	337	2068
8.	351	370	1662	350	370	1546
9.	474	498	1633	474	500	1496
10.	510	535	934	517	537	1195
11.	566	587	1447	564	587	2124

Table 3
Different orientation of the Oatp1b2 protein with TM-scores.

Serial No	Inside to	Outside	Score	Outside	Inside	Score
1.	1	17	**457**	1	17	694
2.	37	56	1010	37	57	1299
3.	65	90	2221	65	86	1930
4.	131	150	**323**	135	162	544
5.	181	200	1898	176	195	1742
6.	224	245	2488	222	238	2647
7.	306	326	2143	305	326	1815
8.	342	363	1629	342	363	1900
9.	368	391	1748	376	396	1732
10.	501	527	2083	438	460	**81**
11.	540	562	821	503	527	2084
12.	–	–	–	539	562	1055

user-friendly interface. It simply reworks the display of selected parts of the protein and assesses distances, angles, and dihedral angles between atoms, including an interactive visual interface that provides an idea of structural motifs and an algorithm for a rapid search from a very large collection of structural databases for motifs in which amino acids are present in core regions [29,33]. Furthermore, the selected amino acids (present outside the core region) were provided to the online server known as the ModLoop Server for the next level of loop refinement [34]. This tool performs automated modeling of loops in protein structures and is based on a technique (as in the MODELLER package) that allows the prediction of loop conformations by optimizing objective functions and satisfaction of spatial restraints without depending on any database [35]. This method augments the positions of all non-hydrogen atoms of a loop in a best-fitted environment. Optimization depends on conjugate gradient minimization and molecular dynamics simulations with simulated annealing. This approach was repeated several times for different stretches of the out-of-core amino acid sequences.

2.3. *Evaluation of the structure quality*

The final prepared model was considered for further studies through multiple refinements of the initially generated protein models. The structural quality of the model, based on stereochemical quality assessment in the Ramachandran plot, was determined using the Rampage tool and PDBsum server for the dihedral angles of different amino acids [32,36]. The Volume Area Dihedral Angle Reporter (VADAR) is a robust tool used for the reliable quality evaluation of peptide and protein structures from their PDB coordinates. The assessment was carried out based on 15 different algorithms/programs and more than 30 structural parameters, such as solvation free energy, local and overall folds, H-bond energy, H-bond partners, steric quality for the whole structure, and single residues of the protein. Different algorithms facilitate the quick identification of problems within newly prepared models [37]. Quality Model Energy Analysis (Q-MEAN) is a tool based on a composite scoring function that correlates with the structure of protein and its major geometrical aspects. This tool uses five structural descriptors for analyzing local geometry by using torsion angle potential over three consecutive amino acids, which is very effective in recognizing the native folds [38].

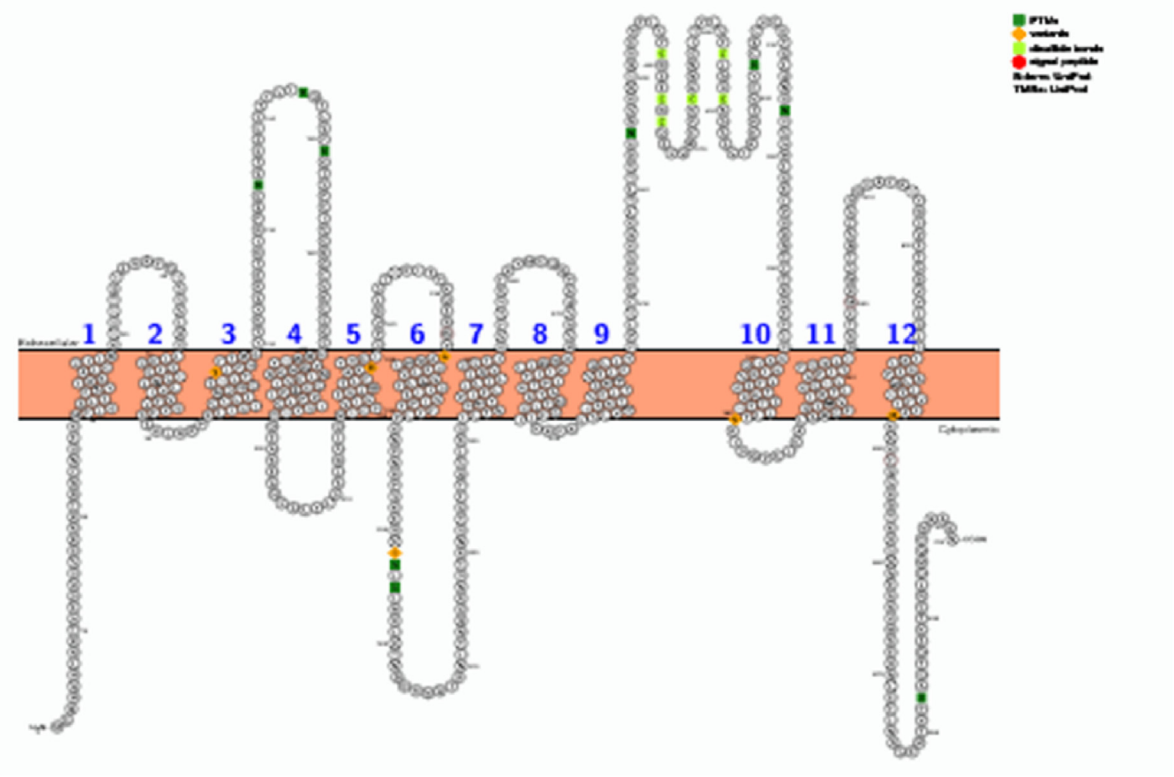

Fig. 6. TM-view for OATP1B3 protein.

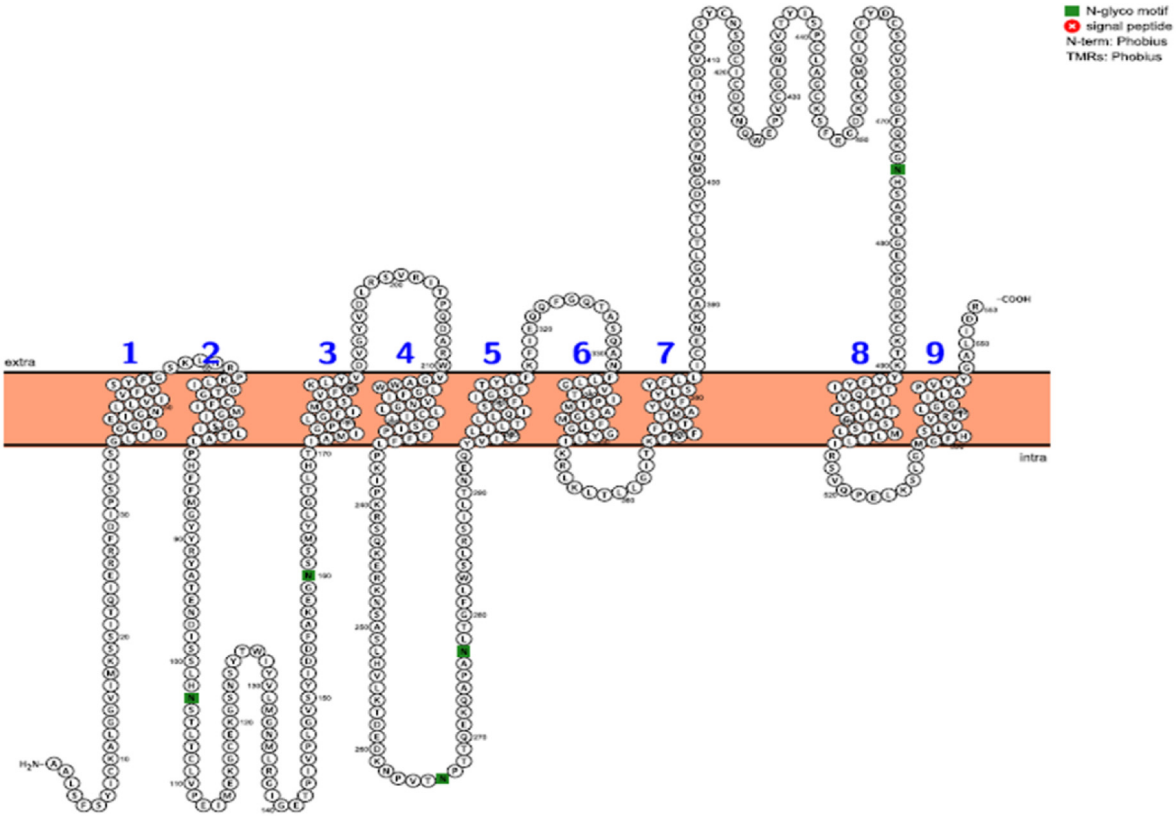

Fig. 7. TM-view for Oatp1b2 protein.

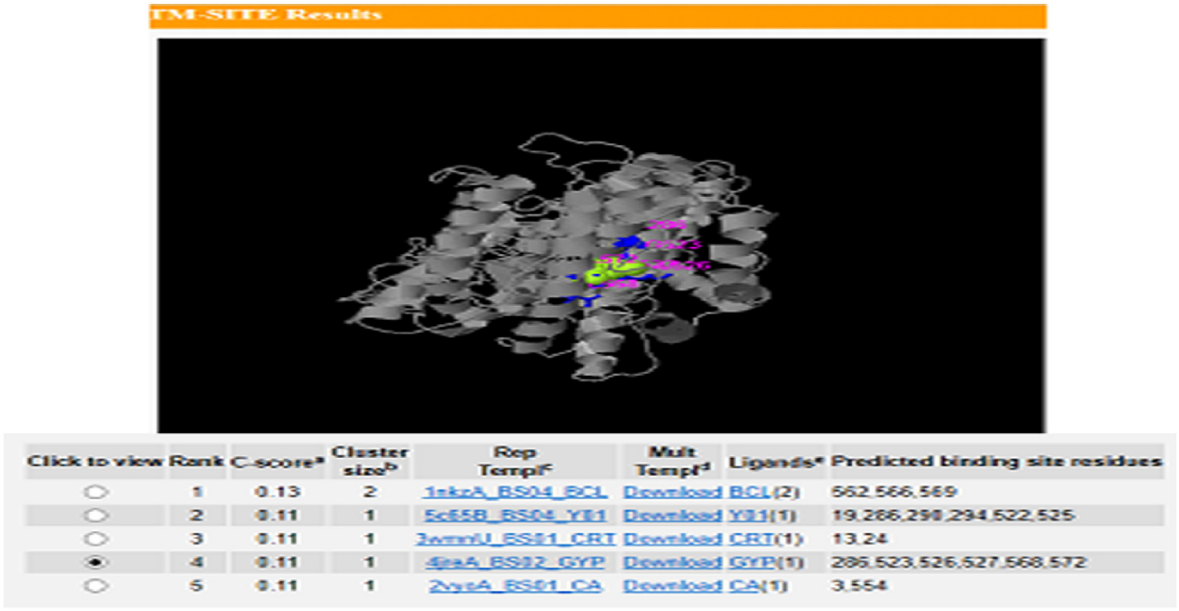

Fig. 8. COACH result for OATP1B3.

Table 4
Protein and ligand docked value showing solution number, global Energy (kcal/mol), attractive VdW (kcal/mol), repulsive (kcal/mol), VdW (kcal/mol) and ACE (kcal/mol) for both the OATP1B3 and Oatp1b2 proteins complexed with MC-LR and quercetin for the best docked structure.

Protein and ligand docked	Solution number	Global energy (kcal/mol)	Attractive VdW (kcal/mol)	Repulsive VdW (kcal/mol)	ACE (kcal/mol)
OATP1B3 and MC-LR	4	−15.6	−41.69	99.38	−26
OATP1B3 and quercetin	8	−39	−17.37	3	−10.37
Oatp1b2 and MC-LR	10	−5.59	−34.39	123.20	−20.9
Oatp1b2 and quercetin	8	−36.40	−16.79	7.32	−10.74

2.4. Modeling the TMPs

Information on the presence and exact location of transmembrane helices is crucial for their functional importance, annotation, and analysis. Several tools were used to validate Oatp1b2 and OATP1B3 as TMPs. The first tool was TMHMM [14]. This method works on a hidden Markov model used for the prediction/prognosis of transmembrane helices and produces results with 97%–98% accuracy for the alpha helix transmembrane region of the protein and also predicts the most probable/accurate location and orientation (overall topology of the protein) of transmembrane helices in the sequence. An algorithm called N-best (or 1-best) sums over all paths of the model with the same location and orientation of the helices. The plot shows the probabilities of the inside/outside/TM helices. The second tool used for transmembrane prediction was TMpred [15]. This program was used to predict membrane-spanning regions and their orientations. The algorithm is based on a statistical assessment of the TMP database, known as TMbase. A combination of different weight matrices for scoring was used to make the predictions. We used the PROTTER [16] online tool for interactive model protein Oatp1b2 data analysis, as well as for hypothesis generation by visualizing both annotated sequence features and experimental proteomic data in relation to protein topology.

2.5. Prediction of drug binding sites

COACH is a robust approach for ligand-binding site (LBS) prediction that syndicates multiple results of different algorithms: TM-SITE, S-SITE, COFACTOR, FINDSITE, and Con Cavity. To make a prediction, a query sequence (Oatp1b2, OATP1B3) in the form of a structure is provided as an input, which runs the individual programs. The top-scoring predictions from each algorithm were combined to provide a predictive consensus stretch of amino acid residues [39]. All of the predicted ligand-binding amino acid residues by the COACH server are undoubted because the ranking of LBS stretch is based on C-scores ranging from 0 (zero) to 1 (one); scores near zero represent random predictions, whereas scores near 1 indicate reliable predictions [40].

2.6. Docking analysis

With model structures (Oatp1b2 and OATP1B3) as receptors and MC-LR as ligands, the next step in the analysis was docking. We used PATCH Dock, an online protein-ligand interaction server, to perform the molecular docking process. This server uses the geometrical shape complementarity method of molecular surfaces to obtain the best-fit model candidate solution [41]. Upload receptor and ligand in its respective place kept default clustering RMSD as 4.0 Å and the complex type was selected as protein-small ligand and then submitted. Subsequently, complementary patches were harmonized to form several docked structures. The top 20 candidate solutions are arranged based on their geometric shape complementarity score (GSC), approximate interface area (AI area), and ACE [41]. Further, all PatchDock solutions were flexibly refined using the FireDock online server to obtain 10 high-throughput solutions. The best-fit docked structure was visualized using Discovery Studio 3.5 software.

3. Results and discussion

3.1. Model prediction, refinement, and structure quality evaluation

In 2006, to predict the structure of GPCR in the human genome, the TASSER method was used over traditional homology modeling

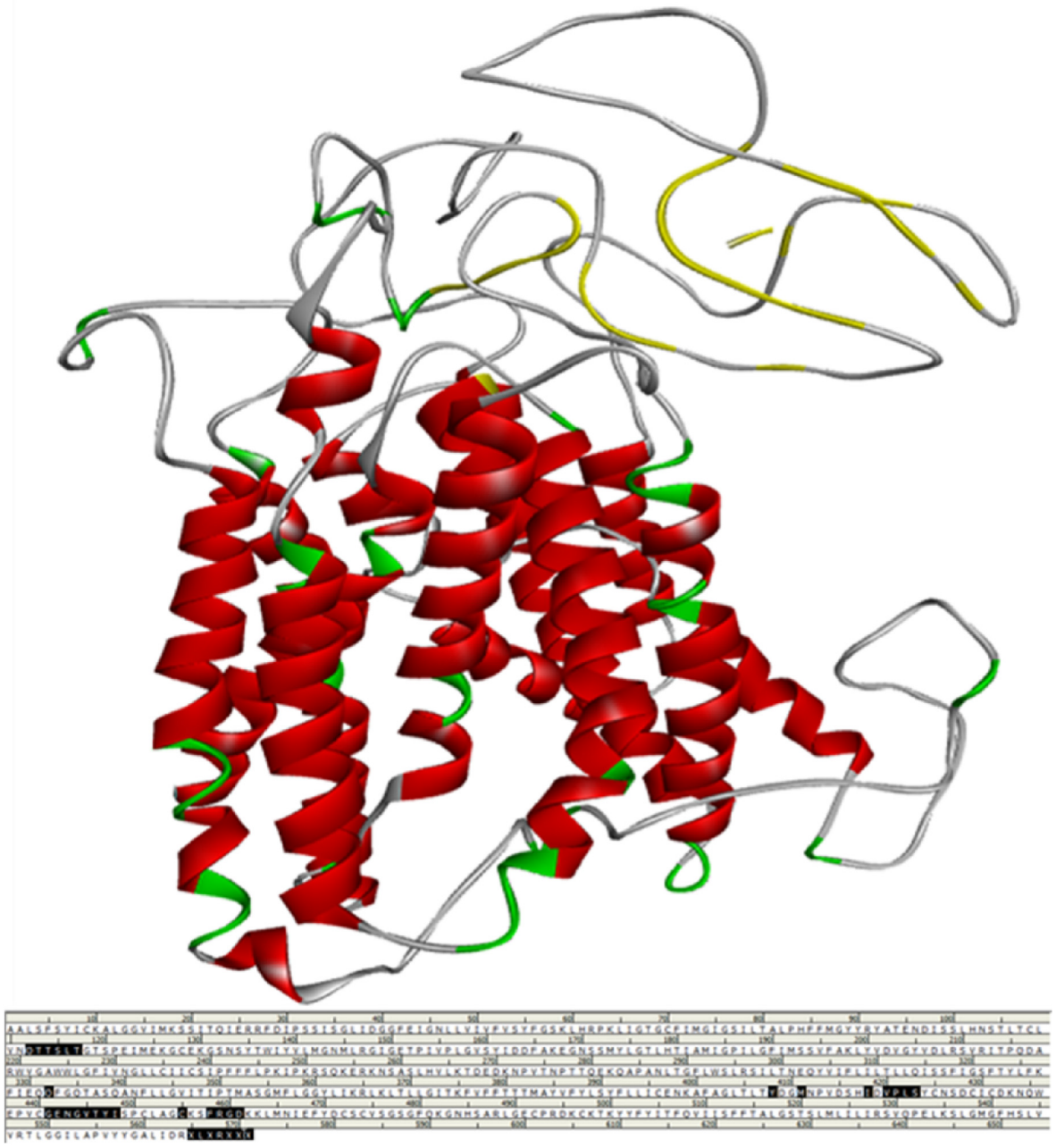

Fig. 9. MC-LR docking site and interacting AAs in OATP1B3.

approaches; TASSER modeling does not require solved homologous template structures; thus, it is able to generate *ab initio* models [42]. An iterative PDB search indicated that the structures of the OATP1B3 and OATB1b2 proteins were not available in this database; therefore, OATP1B3 and OATB1b2 protein structure modeling was performed using the I-TASSER server in a template-independent manner. Its heuristic algorithm, LOMET, searches for appropriate templates from different well-established protein databases to model a robust protein structure [43]. After the OATP1B3and OATB1b2 protein structures were modeled, they were refined using the Mod-refiner tool; however, unfortunately, not all amino acids were present in the allowed region; therefore, there was a need to re-refine models manually with a tool using the Swiss-PDB Viewer and ModLoop server. The PROCHECK program computes several stereochemical parameters for a given protein model and compares them with 'ideal' values obtained from a database of well-refined, high--resolution protein structures in the Protein Data Bank [44]. After several efforts, all of the amino acids were found present in the generously allowed region (100%), and not a single amino acid was present inside the disallowed region (Figs. 1 and 2). Stereochemical quality of the model proteins was evaluated in form of a Ramachandran plot by mean of Procheck server, which showed that the OATP1B3 protein consists of 95% amino acids in its most favored region and 5% in favored region, whereas the Oatp1b2 protein structure has 92.6%amino acids in its most favored region and 7.4% in favored region.

The VADAR tool was then used to evaluate the qualitative and quantitative analyses of the model proteins by predicting several aspects of their secondary structures, hydrogen bond qualities, and volume measurements of the model proteins. The majority of OATP1B3 and Oatp1b2 proteins are mainly composed of coils and helices, but fewer amino acids are involved in beta-helix and turn formation. Three different H-bond measures (observed) of the OATP1B3 and Oatp1b2 proteins did not deviate significantly from their expected values [45], showing that the model protein has a good structure with proper H-bonding along with several helices. For OATP1B3 and Oatp1b2, the

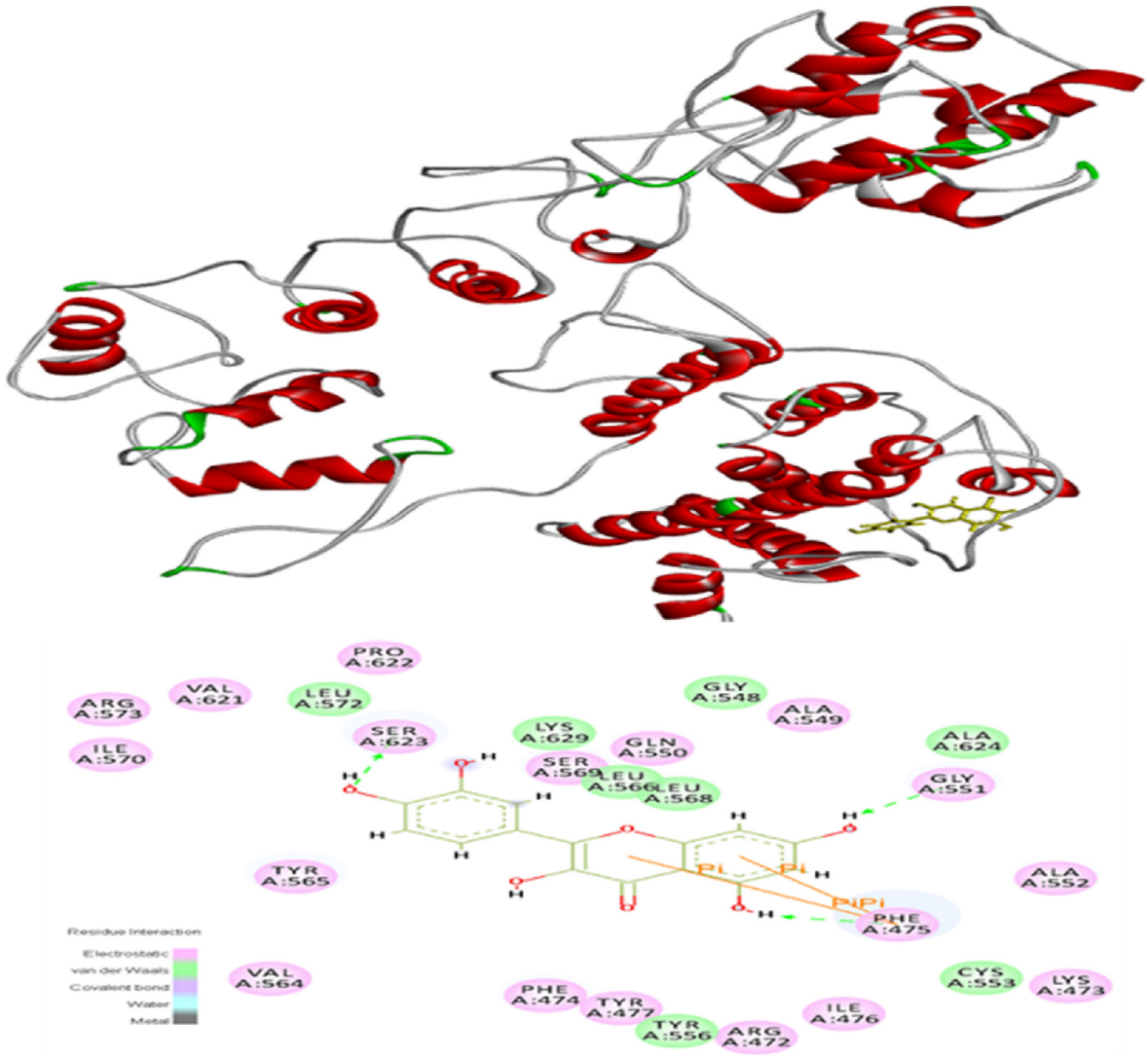

Fig. 10. Quercetin docking site and interacting AAs in OATP1B3.

observed total volume and mean residue volume values were higher than the expected values [46]. In the final VADAR analysis, the molecular weights of the proteins were predicted (Table 1).

Q-MEAN analysis was also performed to authenticate the constructed model structure by analyzing several measures that were set to evaluate the model quality. Normalized Q-MEAN values lie between 0.5 and 1 are considered a good model, and OATP1B3 and Oatp1b2 lie between that limit; hence, they can be accepted as good models. The Z-score value was greater than 2 ($Z > 2$) for OATP1B3 and Oatp1b2 model proteins, and their Q Mean Brain Results show that the models lie between the expected transmembrane region (Figs. 3 and 4).

3.2. Models of TMPs

The authenticated model proteins were used to predict transmembrane domains. Expected trans-membrane "domains" findings have been done by using the most probable topology finder TMHMM which works based on HMM (Hidden Markov Model) algorithm. This tool provided several sets of exact helical boundaries. For OATPAB3, TMHMM predicted 10 TM helices and a small helix that may not be a TM helix, whereas for Oatp1b2, it predicted 9 TM helices and a single small helix. Amino acid stretches were also predicted to indicate the length of the TM-helices (Fig. 5).

3.3. TMpred output for Oatp1b2

TMpred was used to authenticate the number of transmembrane domains. The number of possible transmembrane helices was 11 in the case of inside-to-outside or vice-versa orientation of the OATP1B3 protein, whereas the Oatp1b2 protein had 11 inside-to-outside helices and 12 for outside-to-inside orientation. However, not all helices are TM-helices. According to the TMpred results, only TM helices with scores above 500 were considered significant. Interpretation of the results revealed **10** inside-to outside-oriented TM helices, whereas **11** outside-to inside-oriented TM helices were found in OATP1B3 (Table 2). However, Oatp1b2 has **9** inside to outside oriented and **10** outside to inside oriented TM-helices (Table 3). The TMpred results for the inside-to-outside oriented TM-helices were similar to those obtained using the TMHMM server. These similarities indicate that OATP1B3 has 10 transmembrane helices, and Oatp1b2 has nine transmembrane helices. Both protein structures were confined and well-represented by the Protter tool, which provides pictorial evidence for the geometrical TM view of proteins (Figs. 6 and 7).

3.4. Prediction of drug binding sites

The results obtained for the OATP1B3 from COACH–TM site prediction server indicated the presence of several active sites for ligand binding (Fig. 8). Analysis of all predicted active sites revealed that only

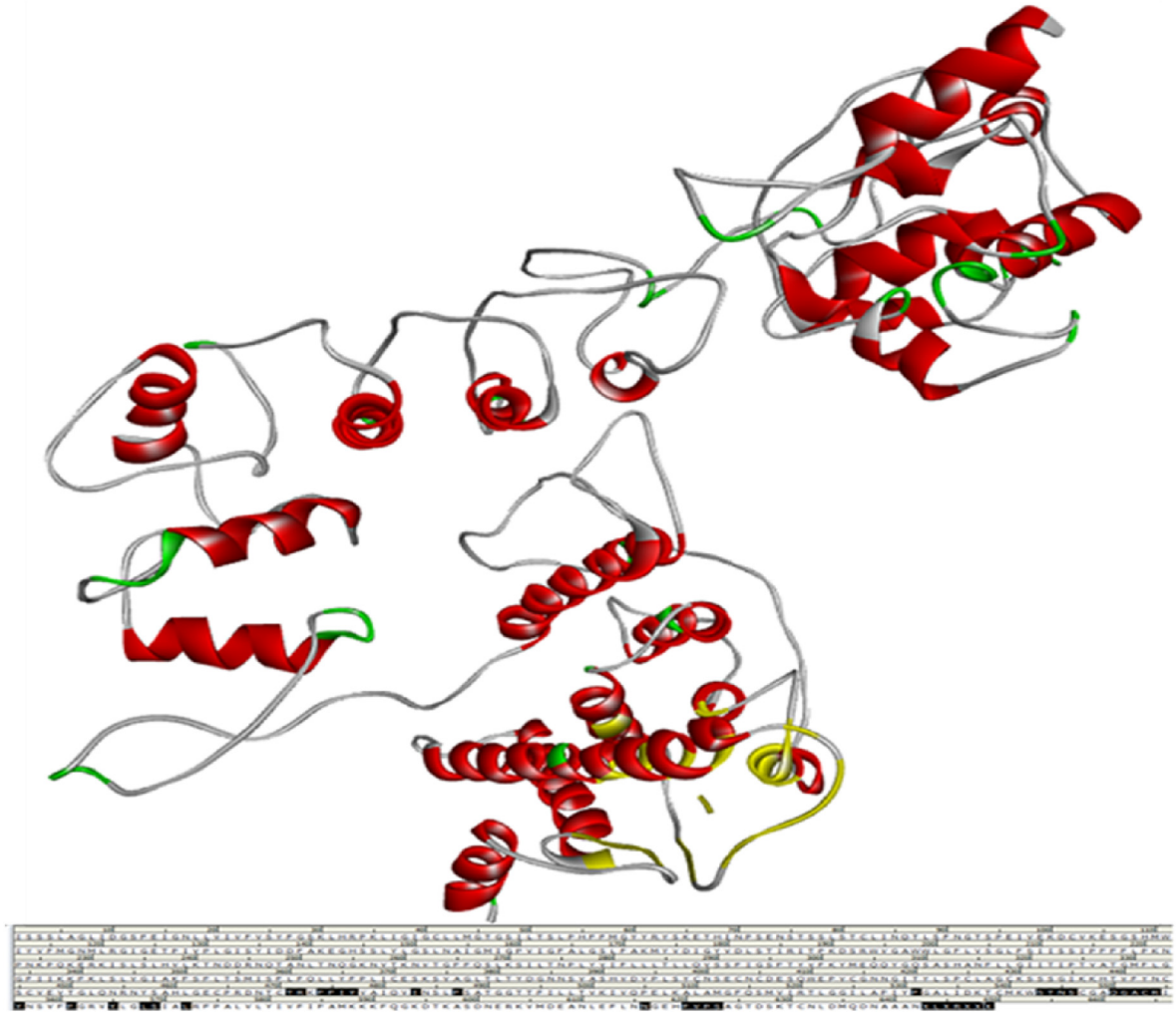

Fig. 11. MC-LR docking site and interacting AAs in Oatp1b2.

two sites with AAs at positions 568, 569, and 572 showed poor interaction with both MC-LR and quercetin. In addition to these three, a few more AAs stretches were common in the interaction with both ligands, which did not lie in the TM-Site predicted range; these were 472–477, 550–552, and 620–623 AAs. Similarly, in the case of Oatp1b2, different active sites were predicted using the COACH & COACH-TM Site prediction servers. Further, on relative analysis of the docked structures of Oatp1b2 with MC-LR or quercetin, we found that either of their interacting AAs coincided with the AAs stretch present in the predicted docking sites. However, the AAs present in stretch 112 to 117 of Oatp1b2 interacted with both MC-LR and quercetin in the individually docked structures.

3.5. Docking analysis

The minimum Global Energy value for any docked structure is recognized for the interpretation and analysis of docking solutions obtained from PatchDock (Solutions) and further redefined by the FireDock (Global Energy) server. Two ligand molecules, MC-LR, a well-known potent hepatotoxin (transported through OATPs), and quercetin, a natural bioactive compound (as an antagonist to transport activity), were used for docking with OATP1B3 and Oatp1b2 (Table 4). For the TMP OATP1B3, the global energy of the eighth solution for quercetin (−39.0 kcal/mol) was significantly less than that of the global energy of the fourth solution for MC-LR (−15.6 kcal/mol) in both docked structures. The steric interaction shows the existence of some AAs in OATP1B3 common to both ligands (Arg472, Phe474, Phe475, Ile476, Tyr477, Gln550, Gly551, Ala552, Cys553, Tyr556, Tyr565, Leu568, Ser569, Leu572, Val621, Pro622, and Ser 623) (Figs. 9 and 10**)**. Similarly, for Oatp1b2, the global energies for both ligands, quercetin eighth solution (−36.4 kcal/mol) and MC-LR tenth solution (−5.59 kcal/mol), were compared (Table 4). The steric interaction showed the existence of some AAs in Oatp1b2 common to both ligands (Gln112, Thr113, Thr114, Ser115, Leu116, and Thr117) (Figs. 11 and 12). The more negative binding energies of transporter proteins docked with the bioactive compound compared to the MC-LR docked structures indicate that quercetin may replace or obstruct the transport of MC-LR. The attractive van der Waals, repulsive van der Waals, and atomic contact energy (ACE) were also predicted.

As reported in a recent study by Tuerkova et al. [47], organic anion transporting polypeptides (OATP1B1, OATP1B3, and OATP2B1) are not usual targets, but they are well recognized for their ability to obstruct and assist with a wide range of drugs, chemicals, or food additives, and can lead to unwanted adverse effects such as liver toxicity and drug-drug or drug-food interactions. They explained the mode of binding of their screened steroid analogs to three different OATPs. Steroid conjugates are recognized as endogenous substrates of these transporters [47]. In a study conducted by Jójárt et al. [48], small chemical structural modifications of estrane derivatives were found to be active in altering their affinity to the OATP2B1 transporter proteinA cyclic L-amino acid heptapeptide analog of Ncp-M1 also inhibits OATP1B1/1B3 transporters, with a higher OATP1B3 preference [49]. OATPs are well known for their

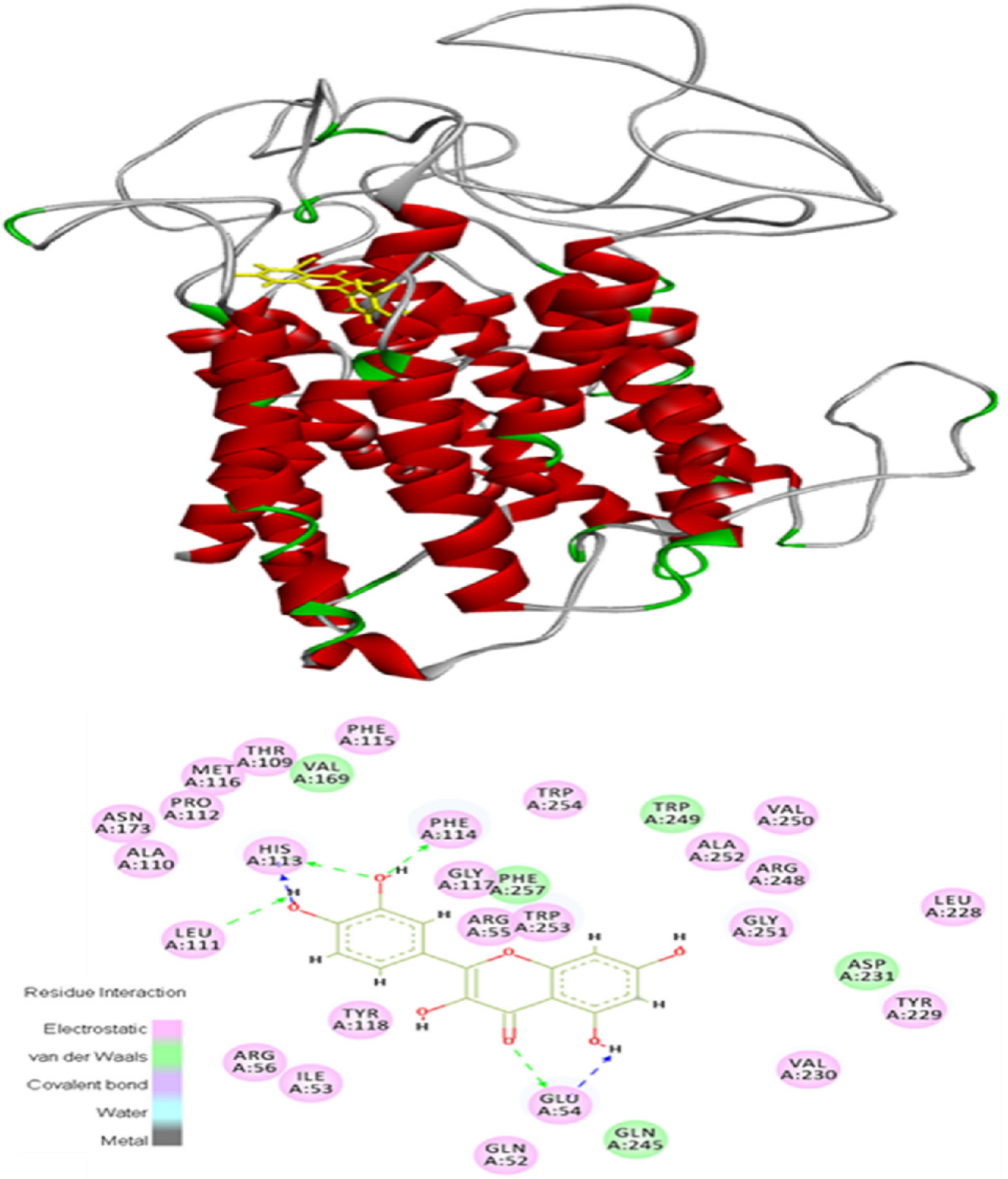

Fig. 12. Quercetin docking site and interacting AAs in Oatp1b2.

participation in pharmacokinetics. Gui et al. [50] in their research described resveratrol and its derivatives as inhibiting the transport of fluorescein methotrexate via OATP1B1 and OATP1B3 [50]. Later, Riha et al. [51] explained the direct transport of resveratrol and its sulfate and glucuronide through OATPs. More recently, in 2022, Poór et al. [52] in their study demonstrated the direct transport of resveratrol by OATPs 1B1, 1B3, and 2B1, confirming the inhibition of OATPs 1B1 and 1B3 by resveratrol. Quercetin is renowned for its positive effects as an antioxidant, anti-inflammatory, and protective agent. Dietary supplements rich in quercetin are widely marketed and show risk of interference with drug therapy in cases of high intake of quercetin [53–55]. The results of pharmacokinetic studies have shown that certain medications are not affected by quercetin, whereas some studies have revealed that a minor dose of quercetin can alter the bioavailability of several drugs [53]. As a result of the oral administration of high doses of quercetin, the values of midazolam decline because of the increased CYP3A4-catalyzed elimination of the drug [56]. Similarly, 500 mg of oral quercetin daily decreased the bioavailability of fexofenadine, presumably because of P-gp inhibition [57].

Nguyen et al. [58] suggested the interactions of quercetin interacts with both efflux (P-gp) and uptake (OATP) transporters, thus inhibiting the OATP-mediated absorption of drugs. Previous studies have shown that quercetin sulfates and glucuronides have potent inhibitory effects on organic anion transporters (OAT1 and OAT3) [59]. The ABC and OATP family transporters are the chief participants in the absorption, distribution, and elimination of a wide range of compounds. Thus, OATP2B1

and OATP1A2 may be involved in the absorption of orally administered flavonoids. Other studies have suggested that quercetin is taken up by Caco-2 and HepG2 cells via OATP2B1 and/or other OATPs (1B1/1B3) [60,61]. Glaeser et al. [62] confirmed the direct cellular uptake of radiolabeled Q in HEK-293 cells. Thus, OATPs 1B1, 1B3, and 2B1 may contribute to the hepatic uptake of flavonoids and their conjugates.

4. Conclusions

Our research was based on computational modeling and docking analyses; accordingly, we focused on investigating the transport of MC-LR through OATPs and assessed the potential of quercetin as a competitive barrier. We successfully modeled OATP1B3 and Oatp1b2 and confirmed the structural quality of their transmembrane helices. Docking analysis demonstrated that quercetin competitively inhibited the binding of MC-LR to target proteins. These findings suggest that quercetin plays a protective role in preventing the translocation of harmful substances. Further research in this area may lead to the development of therapeutic interventions targeting TMP-mediated transport processes. *In vitro* experiments using cultured cells or cell membrane preparations can be used to validate these findings and confirm the inhibitory effect of quercetin on MC-LR transport. Furthermore, animal models could be used to investigate the effects of quercetin on MC-LR toxicity and distribution *in vivo*, there by providing a more comprehensive understanding of its potential protective effects. Furthermore, research into the pharmacokinetic properties, bioavailability, and potential drug-drug interactions of quercetin or its derivatives is critical for its translation into clinical applications. With greater understanding of TMP-mediated toxin transport, new strategies for mitigating toxin-induced damage will arise, ultimately contributing to advancements in toxicology, pharmacology, and therapeutic interventions.

Availability of data and material

The data generated or analyzed during this study are included in this published article. Data will be made available on reasonable request.

Author contributions

Kriti Shrinet & Ritika K Singh: conceptualization and design. Riden Saxena & Avinash K Chaurasia: data analysis and editing help. Arvind Kumar: supervision and final editing.

Funding

DBT to SBT & Sub-Dic Bioinformatics (No.BT/HRD/01/49/2020, Govt. of India), UGC-BHU, UGC-New Delhi-110003.

Ethical approval of studies and informed consent

Though ethical approval of this study is not applicable, the research presented here has been performed in accordance with the Declaration of Helsinki.

Declaration of competing interest

The authors declare that they have no known competing financial interests or personal relationships that could have appeared to influence the work reported in this paper.

Acknowledgements

The authors are thankful to SBT and DBT for providing facilities and initial financial support to carry out the research. KS, RKS, and RS thank UGC-BHU and AKC to UGC-New Delhi for their fellowships. We also thank the Information Officer of the Bioinformatics Center VKS.

References

[1] A. Elofsson, G. von Heijne, Membrane protein structure: prediction versus reality, Annu. Rev. Biochem. 76 (2007) 125–140, https://doi.org/10.1146/annurev.biochem.76.052705.163539.
[2] B. Hagenbuch, P.J. Meier, Organic anion transporting polypeptides of the OATP/SLC21 family: phylogenetic classification as OATP/SLCO superfamily, new nomenclature and molecular/functional properties, Pflügers Archiv 447 (2004) 653–665, https://doi.org/10.1007/s00424-003-1168-y.
[3] T. Mikkaichi, T. Suzuki, T. Onogawa, M. Tanemoto, H. Mizutamari, M. Okada, T. Chaki, S. Masuda, T. Tokui, N. Eto, Isolation and characterization of a digoxin transporter and its rat homologue expressed in the kidney, Proc. Natl. Acad. Sci. USA 101 (2004) 3569–3574, https://doi.org/10.1073/pnas.0304987101.
[4] J. König, Y. Cui, A.T. Nies, D. Keppler, A novel human organic anion transporting polypeptide localized to the basolateral hepatocyte membrane, Am. J. Physiol. Liver Physiol. 278 (2000) G156–G164, https://doi.org/10.1152/ajpgi.2000.278.1.G156.
[5] X. Cheng, J. Maher, C. Chen, C.D. Klaassen, Tissue distribution and ontogeny of mouse organic anion transporting polypeptides (Oatps), Drug Metab. Dispos. (2005) 1062–1073, https://doi.org/10.1124/dmd.105.003640.
[6] W.W. Carmichael, Cyanobacteria secondary metabolites-the cyanotoxins, J. Appl. Bacteriol. 72 (1992) 445–459, https://doi.org/10.1111/j.1365-2672.1992.tb01858.x.
[7] S. Pouria, A. de Andrade, J. Barbosa, R.L. Cavalcanti, V.T.S. Barreto, C.J. Ward, W. Preiser, G.K. Poon, G.H. Neild, G.A. Codd, Fatal microcystin intoxication in haemodialysis unit in Caruaru, Brazil, Lancet 352 (1998) 21–26, https://doi.org/10.1016/s0140-6736(97)12285-1.
[8] W.W. Carmichael, G.L. Boyer, Health impacts from cyanobacteria harmful algae blooms: implications for the North American great lakes, Harmful Algae 54 (2016) 194–212, https://doi.org/10.1016/j.hal.2016.02.002.
[9] N. Bouaïcha, I. Maatouk, Microcystin-LR and nodularin induce intracellular glutathione alteration, reactive oxygen species production and lipid peroxidation in primary cultured rat hepatocytes, Toxicol. Lett. 148 (2004) 53–63, https://doi.org/10.1016/j.toxlet.2003.12.005.
[10] H. Lu, S. Choudhuri, K. Ogura, I.L. Csanaky, X. Lei, X. Cheng, P. Song, C.D. Klaassen, Characterization of organic anion transporting polypeptide 1b2-null mice: essential role in hepatic uptake/toxicity of phalloidin and microcystin-LR, Toxicol. Sci. 103 (2008) 35–45, https://doi.org/10.1093/toxsci/kfn038.
[11] J.P. Overington, B. Al-Lazikani, A.L. Hopkins, How many drug targets are there? Nat. Rev. Drug Discov. 12 (2006) 993–996, https://doi.org/10.1038/nrd2199.
[12] J. Deisenhofer, O. Epp, K. Miki, R. Huber, H. Michel, X-ray structure analysis of a membrane protein complex: electron density map at 3 Å resolution and a model of the chromophores of the photosynthetic reaction center from *Rhodopseudomonas viridis*, J. Mol. Biol. 180 (1984) 385–398, https://doi.org/10.1016/S0022-2836(84)80011-X.
[13] I. Moraes, G. Evans, J. Sanchez-Weatherby, S. Newstead, P.D.S. Stewart, Membrane protein structure determination—the next generation, Biochim. Biophys. ActaBiomembr. 1838 (2014) 78–87, https://doi.org/10.1016/j.bbamem.2013.07.010.
[14] E.P. Carpenter, K. Beis, A.D. Cameron, S. Iwata, Overcoming the challenges of membrane protein crystallography, Curr. Opin. Struct. Biol. 18 (2008) 581–586, https://doi.org/10.1016/j.sbi.2008.07.001.
[15] M. Baker, Making membrane proteins for structures: a trillion tiny tweaks, Nat. Methods 7 (2010) 429–434, https://doi.org/10.1038/nmeth0610-429.
[16] F. Gorrec, Protein crystallization screens developed at the MRC Laboratory of molecular biology, Drug Discov. Today 21 (2016) 819–825, https://doi.org/10.1016/j.drudis.2016.03.008.
[17] K. Lasker, M. Topf, A. Sali, H.J. Wolfson, Inferential optimization for simultaneous fitting of multiple components into a CryoEM map of their assembly, J. Mol. Biol. 388 (2009) 180–194, https://doi.org/10.1016/j.jmb.2009.02.031.
[18] J. Liang, H. Naveed, D. Jimenez-Morales, L. Adamian, M. Lin, Computational studies of membrane proteins: models and predictions for biological understanding, Biochim. Biophys. ActaBiomembr. 1818 (2012) 927–941, https://doi.org/10.1016/j.bbamem.2011.09.026.
[19] T. Nugent, D.T. Jones, Membrane protein structural bioinformatics, J. Struct. Biol. 179 (2012) 327–337, https://doi.org/10.1016/j.jsb.2011.10.008.
[20] H. Koepsell, H. Endou, The SLC22 drug transporter family, Pflügers Archiv 447 (2004) 666–676, https://doi.org/10.1007/s00424-003-1089-9.
[21] V. Buxhofer-Ausch, L. Secky, K. Wlcek, M. Svoboda, V. Kounnis, E. Briasoulis, A.G. Tzakos, W. Jaeger, T. Thalhammer, Tumor-specific expression of organic anion-transporting polypeptides: transporters as novel targets for cancer therapy, J. Drug Deliv. (2013) 1–12, https://doi.org/10.1155/2013/863539.
[22] A.F. Leblanc, J.A. Sprowl, P. Alberti, A. Chiorazzi, W.D. Arnold, A.A. Gibson, K.W. Hong, M.S. Pioso, M. Chen, K.M. Huang, OATP1B2 deficiency protects against paclitaxel-induced neurotoxicity, J. Clin. Invest. 128 (2018) 816–825, https://doi.org/10.1172/JCI96160.
[23] M. Nagai, T. Furihata, S. Matsumoto, S. Ishii, S. Motohashi, I. Yoshino, M. Ugajin, A. Miyajima, S. Matsumoto, K. Chiba, Identification of a new organic anion transporting polypeptide 1B3 mRNA isoform primarily expressed in human cancerous tissues and cells, Biochem. Biophys. Res. Commun. 418 (2012) 818–823, https://doi.org/10.1016/j.bbrc.2012.01.115.
[24] B.A. Wallace, R.W. Janes, in: G. Huether, W. Kochen, T.J. Simat, H. Steinhart (Eds.), Tryptophans in membrane proteins, Tryptophan, Serotonin, and Melatonin, Springer, Boston, MA Link, 1999, pp. 789–799, https://doi.org/10.1007/978-1-4615-4709-9_101.
[25] J. Huang, N. Li, W. Hong, K. Zhan, X. Yu, H. Huang, M. Hong, Conserved tryptophan residues within putative transmembrane domain 6 affect transport function of

organic anion transporting polypeptide 1B1, Mol. Pharmacol. 84 (2013) 521–527, https://doi.org/10.1124/mol.113.085977.
[26] W.C. Rizky, M.C. Jihwaprani, A.A. Kindi, A.N.M. Ansori, M. Mushtaq, The pharmacological mechanism of quercetin as adjuvant therapy of COVID-19, Tradit. Med. Res. 22 (2020) 1–9, https://doi.org/10.53388/life2022-0205-302.
[27] C. Camacho, G. Coulouris, V. Avagyan, N. Ma, J. Papadopoulos, K. Bealer, T.L. Madden, BLAST+: architecture and applications, BMC Bioinf. 10 (2009) 1–9, https://doi.org/10.1186/1471-2105-10-421.
[28] V.K. Vyas, R.D. Ukawala, M. Ghate, C. Chintha, Homology modeling a fast tool for drug discovery: current perspectives, Indian J. Pharmaceut. Sci. 74 (2012) 1–17, https://doi.org/10.4103/0250-474X.102537.
[29] N. Guex, M.C. Peitsch, SWISS-MODEL and the Swiss-Pdb Viewer: an environment for comparative protein modeling, Electrophoresis 18 (1997) 2714–2723, https://doi.org/10.1002/elps.1150181505.
[30] A. Roy, A. Kucukural, Y. Zhang, I-TASSER: a unified platform for automated protein structure and function prediction, Nat. Protoc. 5 (2010) 725–738, https://doi.org/10.1038/nprot.2010.5.
[31] D. Xu, Y. Zhang, Improving the physical realism and structural accuracy of protein models by a two-step atomic-level energy minimization, Biophys. J. 101 (2011) 2525–2534, https://doi.org/10.1016/j.bpj.2011.10.024.
[32] S.C. Lovell, I.W. Davis, W.B. Arendall III, P.I.W. De Bakker, J.M. Word, M.G. Prisant, J.S. Richardson, D.C. Richardson, Structure validation by Cα geometry: ϕ, ψ and Cβ deviation, Proteins: Struct., Funct., Bioinf. 50 (2003) 437–450, https://doi.org/10.1002/prot.10286.
[33] M.U. Johansson, V. Zoete, O. Michielin, N. Guex, Defining and searching for structural motifs using DeepView/Swiss-PdbViewer, BMC Bioinf. 13 (2012) 173, https://doi.org/10.1186/1471-2105-13-173.
[34] A. Fiser, A. Šali, ModLoop: automated modeling of loops in protein structures, Bioinformatics 19 (2003) 2500–2501, https://doi.org/10.1093/bioinformatics/btg362.
[35] A. Fiser, A. Šali, Modeller: generation and refinement of homology-based protein structure models, in: Methods in Enzymology, Department of Biochemistry and Seaver Foundation Center for Bioinformatics, Albert Einstein College of Medicine, Bronz, Elsevier, New York 10461, USA, 2003, pp. 461–491, https://doi.org/10.1016/S0076-6879(03)74020-8.
[36] R.A. Laskowski, E.G. Hutchinson, A.D. Michie, A.C. Wallace, M.L. Jones, J.M. Thornton, PDBsum: a web-based database of summaries and analyses of all PDB structures, Trends Biochem. Sci. 22 (1997) 488–490, https://doi.org/10.1016/s0968-0004(97)01140-7.
[37] L. Willard, A. Ranjan, H. Zhang, H. Monzavi, R.F. Boyko, B.D. Sykes, D.S. Wishart, VADAR: a web server for quantitative evaluation of protein structure quality, Nucleic Acids Res. 31 (2003) 3316–3319, https://doi.org/10.1093/nar/gkg565.
[38] P. Benkert, S.C.E. Tosatto, D. Schomburg, QMEAN: a comprehensive scoring function for model quality assessment, Proteins, Struct. Funct. Bioinforma. 71 (2008) 261–277, https://doi.org/10.1002/prot.21715.
[39] J. Yang, A. Roy, Y. Zhang, Protein–ligand binding site recognition using complementary binding-specific substructure comparison and sequence profile alignment, Bioinformatics 29 (2013) 2588–2595, https://doi.org/10.1093/bioinformatics/btt447.
[40] D.B. Roche, D.A. Brackenridge, L.J. McGuffin, Proteins and their interacting partners: an introduction to protein–ligand binding site prediction methods, Int. J. Mol. Sci. 16 (2015) 29829–29842, https://doi.org/10.3390/ijms161226202.
[41] D. Schneidman-Duhovny, Y. Inbar, R. Nussinov, H.J. Wolfson, PatchDock and SymmDock: servers for rigid and symmetric docking, Nucleic Acids Res. 33 (2005) W363–W367, https://doi.org/10.1093/nar/gki481.
[42] Y. Zhang, M.E. DeVries, J. Skolnick, Structure modeling of all identified G protein–coupled receptors in the human genome, PLoS Comput. Biol. 2 (2006) e13, https://doi.org/10.1371/journal.pcbi.0020013.
[43] S. Wu, Y. Zhang, LOMETS: a local meta-threading-server for protein structure prediction, Nucleic Acids Res. 35 (2007) 3375–3382, https://doi.org/10.1093/nar/gkm251.
[44] R.A. Laskowski, M.W. MacArthur, J.M. Thornton, PROCHECK: Validation of Protein-Structure Coordinates, 2006, https://doi.org/10.1107/97809553602060000882.
[45] A.L. Morris, M.W. MacArthur, E.G. Hutchinson, J.M. Thornton, Stereochemical quality of protein structure coordinates, Proteins: Struct., Funct., Bioinf. 12 (1992) 345–364, https://doi.org/10.1002/prot.340120407.
[46] F.M. Richards, Areas, volumes, packing, and protein structure, Annu. Rev. Biophys. Bioeng. 6 (1977) 151–176, https://doi.org/10.1146/annurev.bb.06.060177.001055.
[47] A. Tuerkova, B.J. Bongers, U. Norinder, O. Ungvári, V. Székely, A. Tarnovskiy, G. Szakács, C. Özvegy-Laczka, G.J.P. van Westen, B. Zdrazil, Identifying novel inhibitors for hepatic organic anion transporting polypeptides by machine learning-based virtual screening, J. Chem. Inf. Model. 62 (2022) 6323–6335, https://doi.org/10.1021/acs.jcim.1c01460.
[48] R. Jójárt, R. Laczkó-Rigó, M. Klement, G. Kőhl, G. Kecskeméti, C. Özvegy-Laczka, E. Mernyák, Design, synthesis and biological evaluation of novel estrone phosphonates as high affinity organic anion-transporting polypeptide 2B1 (OATP2B1) inhibitors, Bioorg. Chem. 112 (2021) 104914, https://doi.org/10.1016/j.bioorg.2021.104914.
[49] L. Herfindal, L. Myhren, R. Kleppe, C. Krakstad, F. Selheim, J. Jokela, K. Sivonen, S.O. Døskeland, Nostocyclopeptide-M1: a potent, nontoxic inhibitor of the hepatocyte drug transporters OATP1B3 and OATP1B1, Mol. Pharm. 8 (2011) 360–367, https://doi.org/10.1021/mp1002224.
[50] C. Gui, A. Obaidat, R. Chaguturu, B. Hagenbuch, Development of a cell-based high-throughput assay to screen for inhibitors of organic anion transporting polypeptides 1B1 and 1B3, Curr. Chem. Genom. 4 (2010) 1–8, https://doi.org/10.2174/1875397301004010001.
[51] J. Riha, S. Brenner, M. Böhmdorfer, B. Giessrigl, M. Pignitter, K. Schueller, T. Thalhammer, B. Stieger, V. Somoza, T. Szekeres, Resveratrol and its major sulfated conjugates are substrates of organic anion transporting polypeptides (OATPs): impact on growth of ZR-75-1 breast cancer cells, Mol. Nutr. Food Res. 58 (2014) 1830–1842, https://doi.org/10.1002/mnfr.201400095.
[52] M. Poór, H. Kaci, S. Bodnárová, V. Mohos, E. Fliszár-Nyúl, S. Kunsági-Máté, C. Özvegy-Laczka, B. Lemli, Interactions of resveratrol and its metabolites (resveratrol-3-sulfate, resveratrol-3-glucuronide, and dihydroresveratrol) with serum albumin, cytochrome P450 enzymes, and OATP transporters, Biomed. Pharmacother. 151 (2022) 113136, https://doi.org/10.1016/j.biopha.2022.113136.
[53] S. Andres, S. Pevny, R. Ziegenhagen, N. Bakhiya, B. Schäfer, K.I. Hirsch-Ernst, A. Lampen, Safety aspects of the use of quercetin as a dietary supplement, Mol. Nutr. Food Res. 62 (2018) 1700447, https://doi.org/10.1002/mnfr.201700447.
[54] R.G. Vida, A. Fittler, A. Somogyi-Végh, M. Poór, Dietary quercetin supplements: assessment of online product informations and quantitation of quercetin in the products by high-performance liquid chromatography, Phytother Res. 33 (2019) 1912–1920, https://doi.org/10.1002/ptr.6382.
[55] A. Miron, A.C. Aprotosoaie, A. Trifan, J. Xiao, Flavonoids as modulators of metabolic enzymes and drug transporters, Ann. N. Y. Acad. Sci. 1398 (2017) 152–167, https://doi.org/10.1111/nyas.13384.
[56] M.A. Nguyen, P. Staubach, S. Wolffram, P.M.A. Langguth, P, The influence of single-dose and short-term administration of quercetin on the pharmacokinetics of midazolam in humans, J. Pharmaceut. Sci. 104 (2015) 3199–3207, https://doi.org/10.1002/jps.24500.
[57] K.-A. Kim, P.-W. Park, J.-Y. Park, Short-term effect of quercetin on the pharmacokinetics of fexofenadine, a substrate of P-glycoprotein, in healthy volunteers, Eur. J. Clin. Pharmacol. 65 (2009) 609–614, https://doi.org/10.1007/s00228-009-0627-6.
[58] M.A. Nguyen, P. Staubach, S. Wolffram, P. Langguth, Effect of single-dose and short-term administration of quercetin on the pharmacokinetics of talinolol in humans–implications for the evaluation of transporter-mediated flavonoid–drug interactions, Eur. J. Pharmaceut. Sci. 61 (2014) 6154–6160, https://doi.org/10.1016/j.ejps.2014.01.003.
[59] C.C. Wong, Y. Akiyama, T. Abe, J.D. Lippiat, C. Orfila, G. Williamson, Carrier-mediated transport of quercetin conjugates: involvement of organic anion transporters and organic anion transporting polypeptides, Biochem. Pharmacol. 84 (2012) 564–570, https://doi.org/10.1016/j.bcp.2012.05.011.
[60] M.N. Chabane, A. Al Ahmad, J. Peluso, C.D. Muller, G. Ubeaud-Séquier, Quercetin and naringenin transport across human intestinal Caco-2 cells, J. Pharm. Pharmacol. 61 (2009) 1473–1483, https://doi.org/10.1211/jpp.61.11.0006.
[61] G. Notas, A.-P. Nifli, M. Kampa, V. Pelekanou, V.-I. Alexaki, P. Theodoropoulos, J. Vercauteren, E. Castanas, Quercetin accumulates in nuclear structures and triggers specific gene expression in epithelial cells, J. Nutr. Biochem. 23 (2012) 656–666, https://doi.org/10.1016/j.jnutbio.2011.03.010.
[62] H. Glaeser, K. Bujok, I. Schmidt, M.F. Fromm, K. Mandery, Organic anion transporting polypeptides and organic cation transporter 1 contribute to the cellular uptake of the flavonoid quercetin, Naunyn-Schmiedeberg's Arch. Pharmacol. 387 (2014) 883–891, https://doi.org/10.1007/s00210-014-1000-6.